Inorg. Chem. **2006**, *45*, 10215–10223

Multinuclear High-Resolution NMR Study of Compounds from the Ternary System NaF–CaF_2–AlF_3: from Determination to Modeling of NMR Parameters

C. Martineau,*,† M. Body,‡ C. Legein,† G. Silly,§ J.-Y. Buzaré,‡ and F. Fayon||

Laboratoire des Oxydes et Fluorures, CNRS UMR 6010, and Laboratoire de Physique de l'Etat Condensé, CNRS UMR 6087, Institut de Recherche en Ingénierie Moléculaire et Matériaux Fonctionnels, CNRS FR 2575, Université du Maine, Avenue O. Messiaen, 72085 Le Mans Cedex 9, France, Laboratoire de Physicochimie de la Matière Condensée, CNRS UMR 5617, Institut Charles Gerhardt, CNRS FR 1878, Université de Montpellier II, Place Eugène Bataillon, CC 03, 34095 Montpellier Cedex 5, France, and Centre de Recherche sur les Matériaux Haute Température, UPR CNRS 4212, 1D Avenue de la Recherche Scientifique, 45071 Orléans Cedex 02, France

Received July 20, 2006

^{27}Al and ^{23}Na NMR satellite transition spectroscopy and 3Q magic-angle-spinning spectra are recorded for three compounds from the ternary NaF–CaF_2–AlF_3 system. The quadrupolar frequency ν_Q, asymmetry parameter η_Q, and isotropic chemical shift δ_{iso} are extracted from the spectrum reconstructions for five aluminum and four sodium sites. The quadrupolar parameters are calculated using the LAPW-based ab initio code WIEN2k. It is necessary to perform a structure optimization of all compounds to ensure a fine agreement between experimental and calculated parameters. By a comparison of experimental and calculated values, an attribution of all of the ^{27}Al and ^{23}Na NMR lines to the crystallographic sites is achieved. High-speed ^{19}F NMR MAS spectra are recorded and reconstructed for the same compounds, leading to the determination of 18 isotropic chemical shifts. The superposition model developed by Bureau et al. is used, allowing a bijective assignment of the ^{19}F NMR lines to the crystallographic sites.

Introduction

Thanks to recent important technological and methodological improvements such as high-speed magic angle spinning (MAS) and high-field, multiquanta MAS (MQMAS), we are now able to accurately extract isotropic chemical shifts and quadrupolar parameters ν_Q (quadrupolar frequency) and η_Q (asymmetry parameter) from the reconstruction of experimental NMR spectra, even for multisite compounds. At present, one of the challenging tasks in solid-state NMR consists of assigning the NMR resonance lines to the corresponding crystallographic sites. One strategy to solve this problem is to precisely calculate the chemical shifts and quadrupolar parameters. This has led, in the past few years, to the development of calculation tools, using either semiempirical or ab initio approaches.

In the case of quadrupolar nuclei, ab initio codes (WIEN2k,[1] ADF,[2] VASP,[3,4] PARATEC,[5] etc.) are able to provide quadrupolar parameters from structural data with good accuracy. The WIEN2k code was proven to be very efficient

* To whom correspondence should be addressed. E-mail: charlotte.martineau.etu@univ-lemans.fr. Fax: 02 43 83 35 06.

† Laboratoire des Oxydes et Fluorures, CNRS UMR 6010, Université du Maine.

‡ Laboratoire de Physique de l'Etat Condensé, CNRS UMR 6087, Université du Maine.

§ Laboratoire de Physicochimie de la Matière Condensée, CNRS UMR 5617, Université de Montpellier II.

|| Centre de Recherche sur les Matériaux Haute Température, UPR CNRS 4212.

(1) Blaha, P.; Schwarz, K.; Masden, G. K. H.; Kvasnicka, D.; Luitz, J. In *WIEN2k. An Augmented Plane Wave + Local Orbitals Program for Calculating Crystal Properties*; Schwarz, K., Ed.; Technische Universität: Wien, Austria, 2001; ISBN 3-9501031-1-2.

(2) te Velde, G.; Bickelhaupt, F. M.; Baerends, E. J.; Fonseca Guerra, C.; van Gisbersen, S. J. A.; Snijders, J. G.; Ziegler, T. *J. Comput. Chem.* **2001**, *22*, 931−967.

(3) Kresse, G.; Hafner, J. *Phys. Rev. B* **1993**, *48*, 13115−13118.

(4) Kresse, G.; Furthmüller, J. *Phys. Rev. B* **1996**, *54*, 11169−11186.

(5) Pfrommer, B.; Raczkowski, D.; Canning, A.; Louie, S. G. *PARATEC* (*PARAllel Total Energy Code*); Lawrence Berkeley National Laboratory (with contributions from Mauri, F.; Cote, M.; Yoon, Y.; Pickard, C.; Heynes, P.): San Francisco, CA.

10.1021/ic061348j CCC: $33.50
Published on Web 11/11/2006

and reliable.[6−18] A key step in the success of these calculations is the optimization of the structures: the atomic positions of the atoms are adjusted, keeping the cell parameters unchanged, until the forces acting on the atoms are minimized. This optimization step is especially important for compounds whose structures were determined from powder diffraction data.[17−20] Finally, by a comparison of experimental and calculated data, a bijective attribution of the NMR resonance lines to the crystallographic sites can be achieved.

^{19}F NMR isotropic chemical shifts can be calculated thanks to a semiempirical superposition model developed by Bureau et al.[21] This model was built for purely ionic fluorides. It assumes that each cation surrounding the studied fluorine anion contributes to the ^{19}F NMR isotropic chemical shift. Body et al.,[22] by refining the model on compounds from the binaries CaF_2-AlF_3 and BaF_2-AlF_3, have previously shown that it can be predictive.[17,22]

In this work, we propose an application of these methods to three compounds from the ternary $NaF-CaF_2-AlF_3$ system: $Na_2Ca_3Al_2F_{14}$,[23] α-$NaCaAlF_6$,[24] and β-$NaCaAlF_6$.[25] In a first step, the experimental quadrupolar parameters ν_Q and η_Q of ^{27}Al and ^{23}Na are extracted from the reconstruction of 3Q-MAS[26,27] and SAtellite TRAnsition Spectroscopy (SATRAS)[28,29] NMR experiments. Next we apply the WIEN2k[1] code to calculate the quadrupolar parameters of these nuclei. A comparison between calculated and experimental values is done, and all of the ^{27}Al and ^{23}Na NMR resonances are assigned to the crystallographic sites. In a second part, ^{19}F NMR isotropic chemical shifts δ_{iso} are determined from the reconstruction of ^{19}F NMR MAS spectra. Then, we make a first assignment of the NMR lines to the crystallographic sites using the superposition model, as was initially proposed by Bureau et al.[21] The agreement is better when using the structures of the compounds optimized with the WIEN2k[1] code.

Materials and Methods

1. Synthesis. Three compounds were observed in the $NaF-CaF_2-AlF_3$ ternary system: $Na_2Ca_3Al_2F_{14}$,[23] $Na_4Ca_4Al_7F_{33}$,[25] and two polymorphic α and β forms of $NaCaAlF_6$.[24,25]

AlF_3, $Na_5Al_3F_{14}$, and $Na_2Ca_3Al_2F_{14}$ always remain as impurities in $Na_4Ca_4Al_7F_{33}$. This compound was not included in our study. Actually, the AlF_3 ^{19}F NMR resonance line matches one of the compound lines, which is a hindrance to accurately determining the relative intensity of this peak. Moreover, in this compound, one sodium cation and one fluorine anion have a site occupancy equal to 0.33 and 0.25, respectively,[25] which prevents us from doing ab initio calculations.

$Na_2Ca_3Al_2F_{14}$[23] and α-$NaCaAlF_6$[24] were synthesized from solid-state reaction of stoichiometric mixtures of NaF, CaF_2, and AlF_3 in sealed platinum tubes. With these starting materials being moisture-sensitive, all operations of weighing, mixing, and grinding were done in a dry glovebox under a nitrogen atmosphere. The corresponding stoichiometric mixtures were heated at 650 °C for 12 h for $Na_2Ca_3Al_2F_{14}$[23] and at 690 °C for 8 days for α-$NaCaAlF_6$ and naturally cooled. The purity of the obtained phases was checked by the X-ray powder diffraction method. CaF_2 is present as an impurity in $Na_2Ca_3Al_2F_{14}$.

β-$NaCaAlF_6$ was obtained from hydrothermal synthesis. CaF_2 and $Na_5Al_3F_{14}$ are present as impurities.

2. NMR Experiments. ^{27}Al ($I = {}^5/_2$) and ^{23}Na ($I = {}^3/_2$) NMR SATRAS spectra were recorded on an Avance 300 Bruker spectrometer (magnetic field $B_0 = 7$ T) using a cross-polarization (CP) MAS probe with either a 4-mm rotor (spinning frequency up to 15 kHz, adapted for small ν_Q) or a 2.5-mm rotor (spinning frequency up to 35 kHz). Under this magnetic field, the Larmor frequencies of ^{27}Al and ^{23}Na are 78.2 and 79.4 MHz, respectively. A 1 M solution of $Al(NO_3)_3$ and a 1 M solution of $Na(NO_3)_3$ were used as external references for ^{27}Al and ^{23}Na, respectively. The linear regime was ensured by using a short pulse duration (1 μs) and a low-radio-frequency (RF) field strength (26 kHz) for both quadrupolar nuclei. The recycle delay was 1 s. Between 4096 and 18 432 free induction decays (FIDs) were accumulated for the ^{27}Al NMR spectra, and between 10 240 and 32 768 FIDs were accumulated for the ^{23}Na NMR spectra. Under these experimental conditions, the relative peak intensities are quantitative. The reconstruction of the SATRAS spectra was achieved using a homemade FORTRAN 95 code based on the theoretical treatment of SATRAS NMR spectra developed by Skibtsted et al.[28,30] and lately corrected.[31,32] The parameters δ_{iso}, ν_Q, and η_Q are extracted from the reconstruction. When several

(6) Iglesias, M.; Schwarz, K.; Blaha, P.; Baldomir, D. *Phys. Chem. Miner.* **2001**, *28*, 67−75.
(7) Tsvyashchenko, A. V.; Fomicheva, L. N.; Magnitskaya, M. V.; Shirani, E. N.; Brudanin, V. B.; Filossofov, D. V.; Kochetov, O. I.; Lebedev, N. A.; Novgorodov, A. F.; Salamatin, A. V.; Korolev, N. A.; Velichkov, A. I.; Timkin, V. V.; Menushenkov, A. P.; Kuznetsov, A. V.; Shabanov, V. M.; Akselrod, Z. Z. *Solid State Commun.* **2001**, *119*, 153−158.
(8) Bastow, T. J. *Chem. Phys. Lett.* **2002**, *354*, 156−159.
(9) Siegel, R.; Hirschinger, J.; Carlier, D.; Ménétrier, M.; Delmas, C. *Solid State Nucl. Magn. Reson.* **2003**, *23*, 243−262.
(10) Bastow, T. J. *Chem. Phys. Lett.* **2003**, *380*, 516−520.
(11) Bastow, T. J.; West, G. W. *J. Phys.: Condens. Matter* **2003**, *15*, 8389−8406.
(12) Corti, M.; Gabetta, A.; Fanciulli, M.; Svane, A.; Christensen, N. E. *Phys. Rev. B* **2003**, *67*, 064416.
(13) Silly, G.; Legein, C.; Buzaré, J.-Y.; Calvayrac, F. *Solid State NMR* **2004**, *25*, 241−251.
(14) Zhou, B.; Giavani, T.; Bildsoe, H.; Skibsted, J.; Jakobsen, H. J. *Chem. Phys. Lett.* **2005**, *402*, 233−238.
(15) Hansen, M. R.; Madsen, G. K.; Jakobsen, H. J.; Skibsted, J. *J. Phys. Chem. A* **2005**, *109*, 1989−1997.
(16) D'Espinose de Lacaillerie, J.-B.; Barberon, F.; Romanenko, K. V.; Lapina, O. B.; Le Pollès, L.; Gautier, R.; Gan, Z. *J. Phys. Chem. B* **2005**, *109*, 14033.
(17) Body, M.; Silly, G.; Legein, C.; Buzaré, J.-Y.; Calvayrac, F.; Blaha, P. *J. Solid State Chem.* **2005**, *178*, 3637−3643.
(18) Body, M.; Silly, G.; Legein, C.; Buzaré, J.-Y.; Calvayrac, F.; Blaha, P. *Chem. Phys. Lett.* **2006**, *424*, 321−326.
(19) Brazdova, V.; Ganduglia-Pirovano, M. V.; Sauer, J. *J. Phys. Chem. B* **2005**, *109*, 394−400.
(20) Hansen, M. R.; Madsen, G. K. H.; Jakobsen, H. J.; Skibsted, J *J. Phys. Chem. B* **2006**, *110*, 5975−5983.
(21) Bureau, B.; Silly, G.; Emery, J.; Buzaré, J.-Y. *Chem. Phys.* **1999**, *249*, 89−104.
(22) Body, M.; Silly, G.; Legein, C.; Buzaré, J.-Y. *Inorg. Chem.* **2004**, *43*, 2474−2485.
(23) Courbion, G.; Ferey, G. *J. Solid State Chem.* **1988**, *76*, 426−431.
(24) Le Bail, A.; Hemon-Ribaud, A.; Courbion, G. *Eur. J. Solid State Inorg. Chem.* **1998**, *35*, 265−272.
(25) Hemon, A.; Courbion, G. *J. Solid State Chem.* **1990**, *84*, 153−164.
(26) Frydman, L.; Hardwood, J. S. *J. Am. Chem. Soc.* **1995**, *117*, 5367−5368.
(27) Medek, A.; Hardwood, J. S.; Frydman, L. *J. Am. Chem. Soc.* **1995**, *117*, 12779−12787.
(28) Skibsted, J.; Nielsen, N. C.; Bildsoe, H. J.; Jakobsen, H. J. *J. Magn. Reson.* **1991**, *95*, 88−117.
(29) Jäger, C., Blümich, B., Eds. *Solid State NMR II*; Springer-Verlag: Berlin, 1994; p 133.

Table 1. Space Groups of the Studied Compounds and Numbers of Fluorine, Aluminum, and Sodium Sites[a]

compound	space group	F	Al	Na
$Na_2Ca_3Al_2F_{14}$	$I2_13$	3 (24c, 24c, 8a)	1 (8a, 3)	1 (8a, 3)
α-$NaCaAlF_6$	$P2_1/c$	12 (4e)	2 (4e, 1)	2 (4e, 1)
β-$NaCaAlF_6$	$P321$	3 (6g)	2 (1a, 32; 2d, 3)	1 (3f, 2)

[a] The Wyckoff multiplicities of the fluorine sites are indicated in parentheses. The Wyckoff multiplicities and site symmetries of the aluminum and sodium sites are indicated in parentheses.

aluminum or sodium sites are present, 3Q-MAS[26,27] experiments were performed prior to the SATRAS spectra. We used the three-pulse *z*-filter[33] sequence and synchronized the experiment with the spinning rate (25 kHz). Signal acquisition was done using the States procedure.[34] Pulse durations to create the triple quantum and the conversion were respectively taken to 2.3 and 0.8 μs for ^{27}Al and 2.8 and 1.1 μs for ^{23}Na with a RF field of 188 kHz for both nuclei. The durations of the selective pulses after the *z* filter were 8 and 14 μs for ^{27}Al and ^{23}Na, respectively. A two-dimensional Fourier transformation followed by a shearing[35] transformation gave a pure absorption two-dimensional spectrum. An estimation of the quadrupolar parameters of each contribution was obtained by reconstructing the corresponding F1 slices with the *Dmfit* software.[36] This allows the reconstruction of the central transition using four adjustable parameters: quadrupolar frequency ν_Q, asymmetry parameter η_Q, isotropic chemical shift δ_{iso}, line width, line shape, and relative line intensity.

Quantitative ^{19}F NMR MAS spectra were acquired either on an Avance 300 Bruker spectrometer (7 T) with a Larmor frequency of 282.2 MHz for ^{19}F or on an Avance 750 Bruker (17.6 T, 705.8 MHz for ^{19}F) spectrometer using a high-speed CP MAS probe with a 2.5-mm rotor. The external reference chosen for isotropic chemical shift determination was C_6F_6 (δ_{iso} C_6F_6 vs $CFCl_3 = -164.2$ ppm[21]). A single t_{90} pulse sequence was applied (4 μs, 61 kHz), followed by the FID acquisition. The delay between two acquisitions was 1 s, ensuring the quantitativity of the spectra. The discrimination of isotropic peaks from side bands was achieved by recording spectra at various spinning rates from 20 to 35 kHz. The ^{19}F NMR spectra were reconstructed using the *Dmfit* software.[36] This allows a full reconstruction of the spectra (including the spinning side bands) with six adjustable parameters: isotropic chemical shift δ_{iso}, chemical shift anisotropy δ_{aniso}, chemical shift asymmetry parameter η_{CS}, line width, relative line intensity, and line shape. δ_{iso}, δ_{aniso}, η_{CS}, relative line intensity, and line shape were assumed to be independent of the spinning rate.

Results

1. ^{27}Al and ^{23}Na NMR. $Na_2Ca_3Al_2F_{14}$ presents one aluminum site and one sodium site (Table 1). Its structure consists of isolated AlF_6^{3-} octahedra, between which 8-fold calcium, 7-fold sodium, and "free" fluorine ions are inserted.[23] The ^{27}Al and ^{23}Na NMR SATRAS spectra are shown in Figure 1. One aluminum site and one sodium site are evidenced, according to the structure. The central transition of the ^{27}Al NMR spectrum is shapeless, characteristic of small ν_Q and $\eta_Q = 0$. The full SATRAS spectrum allows one to determine $\nu_Q = 65$ kHz from the shape of the spinning-side-band envelope. The central transition of the ^{23}Na NMR spectrum is reconstructed with the following parameters: $\delta_{iso} = 5$ ppm, $\nu_Q = 1680$ kHz, and $\eta_Q = 0$. The null η_Q values are in agreement with the axial symmetry of the aluminum and sodium sites.

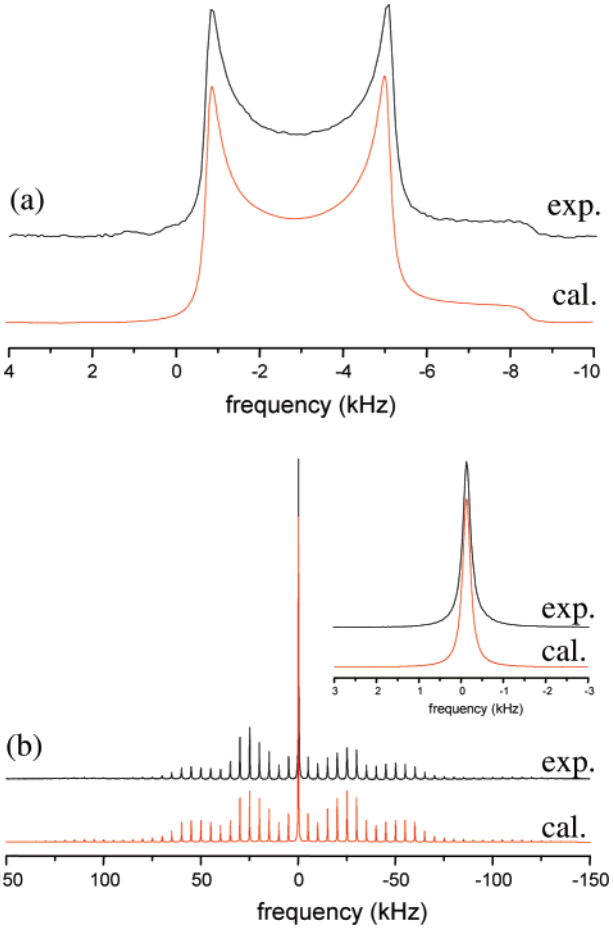

Figure 1. (a) Experimental and calculated central transitions of the ^{23}Na NMR SATRAS spectra of $Na_2Ca_3Al_2F_{14}$ recorded at a spinning rate of 5 kHz. (b) Experimental and calculated ^{27}Al NMR SATRAS spectra recorded at a spinning rate of 10 kHz. The shapeless central transition of the ^{27}Al NMR spectrum is presented in inset.

α-$NaCaAlF_6$ presents two aluminum and two sodium sites with the same multiplicity 4e (Table 1). The structure consists of two types of isolated AlF_6^{3-} octahedra, between which 7-fold calcium and 7-fold and 8-fold sodium cations are inserted.[24] The ^{27}Al NMR 3Q-MAS spectrum does not allow resolution of the two aluminum sites and is therefore not shown. Two contributions with equal intensities are needed to reproduce the characteristic shape of the experimental SATRAS spectrum (Figure 2). The parameters are (i) $\delta_{iso} = -2.6$ ppm, $\nu_Q = 570$ kHz, and $\eta_Q = 0.25$ and (ii) $\delta_{iso} = -3$ ppm, $\nu_Q = 440$ kHz, and $\eta_Q = 0.10$. The closeness of the

(30) Skibsted, J.; Nielsen, N. C.; Bildsoe, H.; Jakobsen, H. J. *Chem. Phys. Lett.* **1992**, *188*, 405−412.
(31) Ding, S.; McDowell, C. A. *Chem. Phys. Lett.* **2001**, *333*, 413−418.
(32) Scholz, G.; Stösser, R.; Klein, J.; Buzaré, J.-Y.; Silly, G.; Laligant, Y.; Ziemer, B. *J. Phys.: Condens. Matter.* **2002**, *14*, 2101−2117.
(33) Amoureux, J. P.; Fernandez, C.; Steuernagel, S. *J. Magn. Reson.* **1996**, *123*, 116−118.
(34) States, D.; Haberkorn, R.; Ruben, D. *J. Magn. Reson.* **1982**, *48*, 286−292.
(35) Ernst, R.; Bodenhausen, G.; Wokaun, A. *Principles of Nuclear Magnetic Resonance in One and Two Dimensions*; Oxford University Press: New York, 1987.
(36) Massiot, D.; Fayon, F.; Capron, M.; King, I.; Le Calvé, S.; Alonso, B.; Durand, J.-O.; Bujoli, B.; Gan, Z.; Hoatson, G. *Magn. Reson. Chem.* **2002**, *40*, 70−76.

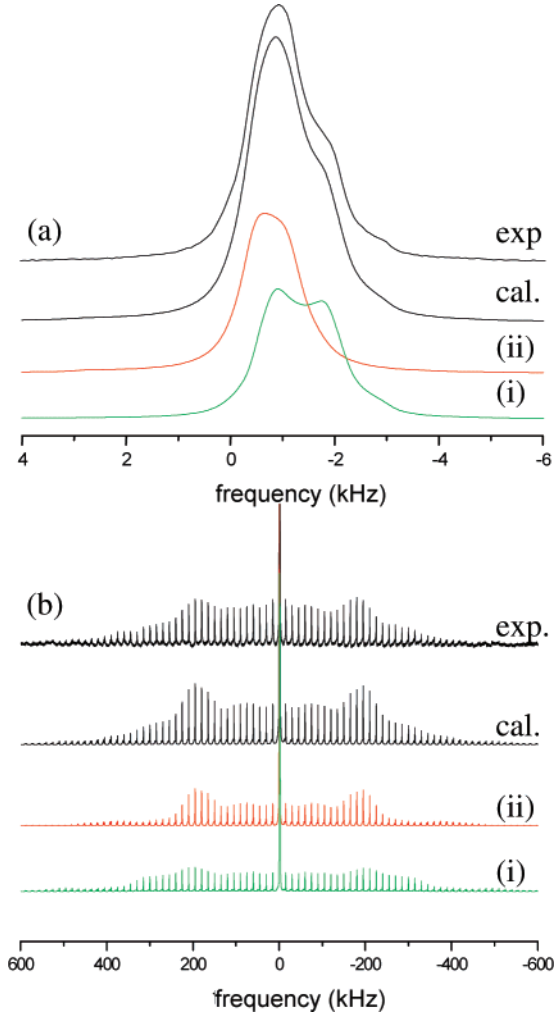

Figure 2. Experimental and calculated (a) central transitions and (b) full ^{27}Al NMR SATRAS spectrum of α-$NaCaAlF_6$ recorded at a spinning rate of 9 kHz. In the full SATRAS spectrum, the central transition is truncated to improve the reflection of the spinning-side-band intensities. The calculated spectrum corresponds to the summation of contributions i and ii of the two aluminum sites.

parameters explains why the two resonances are not resolved in the ^{27}Al NMR 3Q-MAS spectrum. The F1 dimension of the ^{23}Na NMR 3Q-MAS spectrum (Figure 3) clearly evidences two sites, as was expected from the structure. A first estimation of the quadrupolar parameters is done by reconstructing the F1 slices corresponding to the two components: (i) $\nu_Q = 700$ kHz and $\eta_Q = 0.80$ and (ii) $\nu_Q = 1180$ kHz and $\eta_Q = 0.95$. Two contributions of equal intensity allow the reconstruction of the central transition of the ^{23}Na NMR SATRAS spectrum (Figure 4). The quadrupolar parameters are (i) $\nu_Q = 680$ kHz and $\eta_Q = 0.80$ and (ii) $\nu_Q = 1170$ kHz and $\eta_Q = 0.95$, close to the values estimated from the 3Q-MAS spectrum. Because the two aluminum and two sodium sites have the same multiplicity, no attribution can be performed at this stage.

β-$NaCaAlF_6$ presents two aluminum sites with respective multiplicities 1a and 2d and one sodium site (Table 1). The structure consists of either corner-linked or edge-linked AlF_6^{3-}, CaF_6^{4-}, and NaF_6^{5-} octahedra.[25] The two aluminum contributions are not resolved on the ^{27}Al NMR 3Q-MAS spectrum, which is therefore not shown. The ^{27}Al NMR SATRAS spectrum and the central transition of the ^{23}Na NMR SATRAS spectrum are shown in Figure 5. As was previously mentioned, $Na_5Al_3F_{14}$ is present as an impurity in the sample. Its structure shows two aluminum and two sodium sites.[37] The two ^{23}Na lines are clearly evidenced on the ^{23}Na NMR SATRAS spectrum (Figure 5). These contributions were reconstructed using the NMR parameter values previously determined by Silly et al.[13] An estimation of the molar proportion of the impurity in the sample could be deduced: 4%. In the ^{27}Al NMR spectrum, the impurity is not seen, hidden under the contributions of β-$NaCaAlF_6$. However, it was taken into account for the reconstruction of the full ^{27}Al NMR SATRAS spectrum, with the proportion determined from the ^{23}Na NMR spectrum and using the relevant NMR parameters previously determined by Silly et al.[13] Finally, the best reconstruction for β-$NaCaAlF_6$ was obtained with two contributions of respective relative intensities 33% and 67%, in agreement with structural data. On the basis of the relative intensities, the first contribution was assigned to Al1 and the second one to Al2. The parameters are $\nu_Q = 195$ kHz and $\eta_Q = 0$ for Al1 and $\nu_Q = 60$ kHz and $\eta_Q = 0$ for Al2. Both contributions have the same $\delta_{iso} = -3$ ppm. The identical δ_{iso} and η_Q values explain why the two lines are not resolved in the ^{27}Al NMR 3Q-MAS spectrum. The null ^{27}Al η_Q parameters are in agreement with the axial symmetry of the aluminum sites. The central transition of the ^{27}Al NMR SATRAS spectrum is shapeless and is not shown. The ^{23}Na NMR SATRAS spectrum was reconstructed with one contribution for β-$NaCaAlF_6$. The quadrupolar parameters are $\nu_Q = 65$ kHz and $\eta_Q = 1$. This latter value is characteristic of a fully rhombic symmetry.

The reconstruction parameters δ_{iso}, ν_Q, and η_Q are listed in Table 2. One can notice that the ^{27}Al δ_{iso} values are characteristic of an aluminum cation in 6-fold coordination.

2. ^{19}F NMR. $Na_2Ca_3Al_2F_{14}$ presents three fluorine sites, F1, F2, and F3, with respective multiplicities 24c, 24c, and 8a (Table 1). Three lines with respective intensities 43, 43, and 14% are expected. The spectrum shows four lines (Figure 6a). The line at 58 ppm is attributed to CaF_2.[21] The three remaining lines are at +42, +16, and −5 ppm, with respective intensities 14, 43, and 43%. With respect to the site multiplicities, only the 42 ppm line could surely be attributed to F3. The isotropic chemical shifts and relative intensities are gathered in Table 3.

α-$NaCaAlF_6$ presents 12 fluorine sites of the same multiplicity[24] (Table 1). So, 12 resonance lines with the same intensity are expected. The ^{19}F NMR spectrum recorded on the 7-T spectrometer evidences seven NMR lines (Figure 6d). We recorded a spectrum on a higher field spectrometer (17.6 T; Figure 6c). The line resolution is better, the isotropic chemical shifts are more accurately determined, but the magnetic field is not strong enough to resolve the 12 lines. This latter spectrum was reconstructed with eight lines. Lines 2, 4, and 6−8 correspond to one fluorine site, lines 1 and 5 each correspond to two fluorine sites, and line 3 corresponds

(37) Jacoboni, C.; Leblé, A.; Rousseau, J.-J. *J. Solid State Chem.* **1981**, *36*, 297−304.

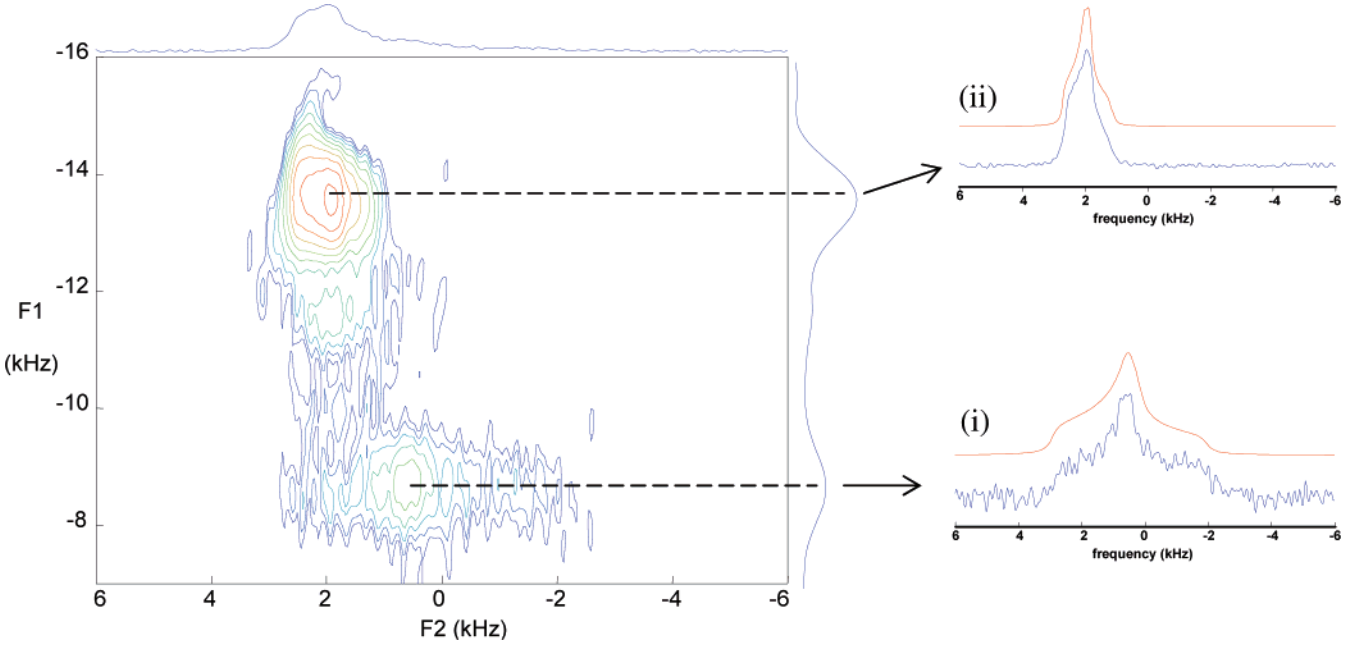

Figure 3. Experimental ^{23}Na NMR 3Q-MAS spectrum of α-$NaCaAlF_6$ at 25 kHz. Top and right curves are the projections on MAS (F2) and isotropic (F1) axes, respectively. On the right side are presented the slices extracted from the ^{23}Na NMR 3Q-MAS spectrum corresponding to the first (i) and second (ii) experimental and reconstructed components along the F1 axis.

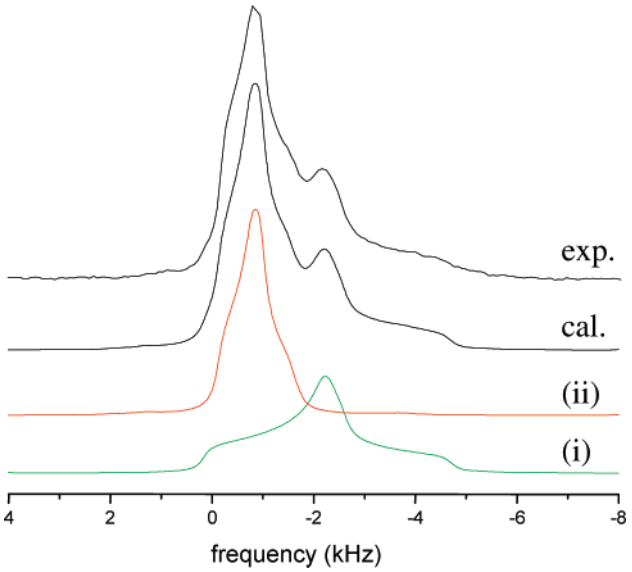

Figure 4. Central transition of the ^{23}Na NMR SATRAS spectrum of α-$NaCaAlF_6$ at 25 kHz. The calculated spectrum corresponds to the summation of the contributions i and ii for the two sodium sites.

to three fluorine sites. Because all of the fluorine sites have the same multiplicity, no line attribution can be deduced from the spectrum. The chemical shifts and relative intensities of the lines are gathered in Table 3.

β-$NaCaAlF_6$ presents three fluorine sites with the same multiplicity (Table 1). The ^{19}F NMR spectrum recorded on the 7-T spectrometer (not shown) evidences four resonance lines from −25 to +58 ppm. The 58 ppm line is attributed to CaF_2[21] identified as an impurity. $Na_5Al_3F_{14}$, contained as an impurity in the sample, has three fluorine sites,[37] whose δ_{iso} values were previously determined at −25, −23, and +3 ppm for F1, F3, and F2, respectively.[38] So, the −25 and −23 ppm lines found on the ^{19}F NMR spectrum were attributed to the F1 and F3 fluorine atoms of $Na_5Al_3F_{14}$. Because those two lines are isolated, we could deduce the intensity of the third line. The intensities of the lines confirm the molar proportion of the impurity in the sample deduced from the ^{23}Na NMR SATRAS spectrum: 4%. The full contribution of $Na_5Al_3F_{14}$ was so taken into account for the reconstruction of the spectrum. Finally, only one line remains for *β*-$NaCaAlF_6$. A better resolution was obtained by recording a spectrum on a higher field spectrometer (17.6 T; Figure 6b). Two lines at 6 and 13 ppm with respective relative intensities 63% and 37% are set for *β*-$NaCaAlF_6$. Because the three fluorine sites have the same multiplicity, we were not able to assign the lines to the fluorine sites. The chemical shifts and relative intensities of the lines are gathered in Table 3.

On the basis of only the different multiplicities, only one line attribution could be performed in the three studied compounds.

Discussion

To correlate NMR resonances and crystallographic sites, NMR parameter calculations were carried out.

1. ^{27}Al and ^{23}Na NMR Quadrupolar Parameter ab Initio Calculations. Ab initio calculations of ^{27}Al and ^{23}Na electric field gradients (EFGs) were performed using the WIEN2k code,[1] which is a full potential (linearized) augmented plane wave code for periodic systems. Atomic sphere sizes of 1.6, 1.65, 1.8, and 1.65 au were used for fluorine, sodium, calcium, and aluminum, respectively, for all compounds except for α-$NaCaAlF_6$, whose fluorine sphere size was taken to be 1.55 au. The basis set was determined by a large cutoff corresponding to $R_{MT}K_{max} = 8$ (about 5800 plane

(38) Body, M.; Silly, G.; Legein, C.; Buzaré, J.-Y. *J. Phys. Chem. B* **2005**, *109*, 10270−10278.

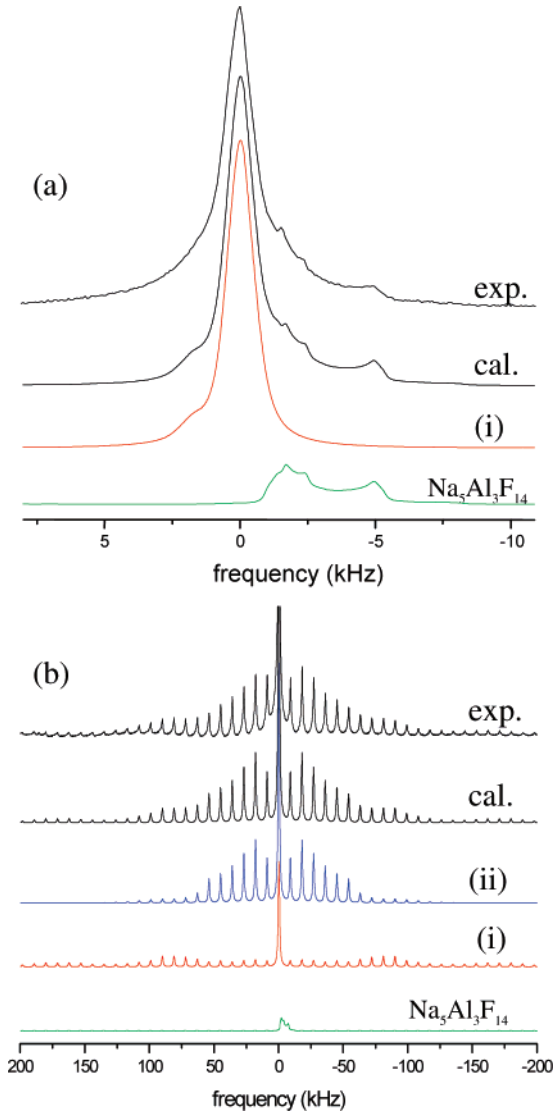

Figure 5. (a) Experimental and calculated central transitions of the ^{23}Na NMR SATRAS spectrum of β-$NaCaAlF_6$ recorded at 25 kHz. The calculated spectrum corresponds to the summation of the contributions of the sodium site of β-$NaCaAlF_6$ (i) and the two sodium sites of $Na_5Al_3F_{14}$. (b) Experimental and calculated ^{27}Al NMR full SATRAS spectra of β-$NaCaAlF_6$ recorded at 9 kHz. The calculated spectrum corresponds to the summation of the contributions i and ii of the two aluminum sites of β-$NaCaAlF_6$ and the contributions of $Na_5Al_3F_{14}$. In the full ^{27}Al NMR SATRAS spectrum, the central transition is truncated to improve the reflection of the spinning-side-band intensities.

waves). The full Brillouin zone was sampled with 100 k points, and we used the generalized gradient approximation of Perdew et al.[39] for the description of exchange and correlation effects within the density functional theory. First the structures were optimized by adjusting the atomic positions, keeping the experimental cell parameters unchanged, until the forces acting on all atoms were reduced to below 2 mRy/au.

1.1. Effects of the Structure Optimizations. The optimized structures of $Na_2Ca_3Al_2F_{14}$ and β-$NaCaAlF_6$ are similar to the initial ones (see the Supporting Information). However, the atomic positions of the optimized structure of α-$NaCaAlF_6$ are more affected: shifts of the atomic positions of F atoms up to 0.176 Å are observed (see the Supporting Information). In this compound, the optimization effects can be followed by the evolution of the radial and angular distortions of the AlF_6^{3-} octahedra and by the M−F (M = Al, Ca, Na) and F−F distance variations. The octahedral distortions are characterized by three parameters: the root-mean-square (rms) deviation from the mean M−F (M = Al, Na, Ca) distance d_m (also called radial distortion), $\Delta d = \sqrt{\sum_{i=1}^{6}(d_i - d_m)/6}$ with $d_m = \sqrt{\sum_{i=1}^{6} d_i/6}$, the rms deviation from 90° for the F−M−F angles between two adjacent M−F bonds (angular distortion), $\Delta\theta_\perp = \sqrt{\sum_{i=1}^{12}(\theta_i - 90)/12}$, and the rms deviation from 180° for the F−M−F angles between two opposite M−F bonds (angular distortion), $\Delta\theta_{||} = \sqrt{\sum_{i=1}^{3}(\theta_i - 180)/3}$. The radial and angular distortions before and after optimization are gathered in Table 4. Because the Ca−F and Na−F distance variations are not significant, they are not discussed. The main optimization effect is the reduction of the AlF_6^{3-} octahedron distortions, which were initially notably distorted. In the initial structures, the Al−F distances range from 1.709 to 1.903 Å, respectively too short and too long with regard to the sum of the ionic radii[40] of the 6-fold aluminum cation and fluorine anion, which is equal to 1.820 Å. In the optimized structures, the minimum Al−F distance is 1.779 Å and the maximum 1.859 Å. F−F distances as short as 2.249 Å are also observed in the initial structure of α-$NaCaAlF_6$,[24] when the sum of two ionic radii of the fluorine anion is 2.570 Å.[40] The minimum F−F distances are more reasonable after optimization: 2.480 Å. Therefore, the structure of α-$NaCaAlF_6$ optimized with WIEN2k seems to be crystallographically more satisfactory. This trend, i.e., the reduction of the AlF_6^{3-} octahedron distortions, was previously observed by Body et al.[17,18] on two compounds whose structures were determined from X-ray powder diffraction data. Although the structure of β-$NaCaAlF_6$ was also determined from X-ray powder diffraction data, the optimization effects are quite small (shifts of the atomic positions of F atoms smaller than 0.044 Å). This can be explained by the fact that this compound has only 11 atomic coordinates to be refined (see the Supporting Information), which leads to more precise values. The small variations of the atomic positions in $Na_2Ca_3Al_2F_{14}$ (≤0.017 Å) are consistent with the fact that the structure, determined from X-ray crystal diffraction data, was accurate.

1.2. Quadrupolar Parameter Calculations. The EFG tensor characterizes the distribution of the electronic charge surrounding a nucleus. For a nucleus with a spin $I > 1/2$, the quadrupolar frequency ν_Q and the asymmetry parameter η_Q are related to the components of the EFG tensor through the following equations: $\nu_Q = 3eV_{zz}Q/2I(2I - 1)h$ and $\eta_Q = (V_{xx} - V_{yy})/V_{zz}$.

The corresponding quadrupolar frequencies are calculated from the V_{zz} component using the nuclear quadrupole moment reported by Pyykkö:[41] $Q(^{27}Al) = 1.466 \times 10^{-29}$ m^2 and $Q(^{23}Na) = 1.04 \times 10^{-29}$ m^2. Because the NMR spectrum

(39) Perdew, J. P.; Burke, K.; Ernzerhof, M. *Phys. Rev. Lett.* **1996**, *77*, 3865−3968.
(40) Shannon, R. D. *Acta Crystallogr.* **1976**, *A32*, 751−767.
(41) Pyykkö, P. *Mol. Phys.* **2001**, *99*, 1617−1629.

Table 2. Experimental Isotropic Chemical Shifts $\delta_{iso,exp}$ (ppm), Quadrupolar Frequencies $\nu_{Q,exp}$ (kHz), Asymmetry Parameters $\eta_{Q,exp}$, and Calculated V_{zz} ($V\ m^{-2}$), $\nu_{Q,cal}$ (kHz), and $\eta_{Q,cal}$ for All of the ^{27}Al and ^{23}Na of the Studied Compounds[a]

compound	contribution	$\delta_{iso,exp}$	$\nu_{Q,exp}$ (±50 kHz)	$\eta_{Q,exp}$ (±0.1)	V_{zz}	$\nu_{Q,cal}$	$\eta_{Q,cal}$	attribution
$Na_2Ca_3Al_2F_{14}$	Al	−1.6	65	0	1.33×10^{20}	70	0	Al1
	Na	5.2	1680	0	-1.32×10^{21}	1655	0	Na1
α-$NaCaAlF_6$	Al (i)	−3.4	570	0.25	9.80×10^{20}	520	0.24	Al1
	Al (ii)	−2.2	440	0.1	-7.61×10^{20}	404	0.11	Al2
	Na (i)	2.0	1170	0.95	-9.91×10^{20}	1242	0.94	Na2
	Na (ii)	−1.6	680	0.80	5.84×10^{20}	732	0.77	Na1
β-$NaCaAlF_6$	Al (i)	−3	195	0	3.74×10^{20}	198	0	Al1
	Al (ii)	−3	60	0	1.04×10^{20}	55	0	Al2
	Na	7	600	1	4.80×10^{20}	600	0.98	Na1

[a] The attribution of the site is presented in the last column.

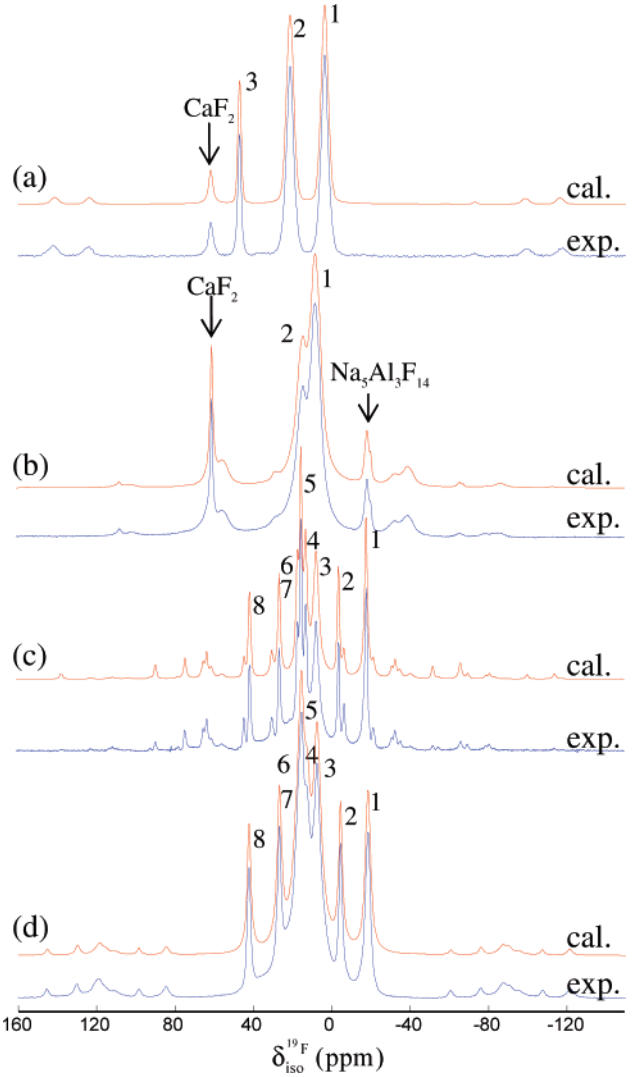

Figure 6. ^{19}F NMR MAS spectra recorded at 7 T at 35 kHz of (a) $Na_2Ca_3Al_2F_{14}$ and (d) α-$NaCaAlF_6$. ^{19}F NMR MAS spectra recorded at 17.6 T at 34 kHz of (c) α-$NaCaAlF_6$ and (b) β-$NaCaAlF_6$. The remaining unnumbered lines are the spinning side bands. The impurities are identified by their name.

is not sensitive to the sign of ν_Q at room temperature, only absolute values of V_{zz} are considered.

As was previously observed,[17,18] the calculated EFG components can vary significantly after optimization of the structures. For example, the calculated V_{zz} and η_Q values for Al1 in α-$NaCaAlF_6$ goes from -7.9×10^{20} V m^{-2} and 0.95, respectively, for the initial structure to 9.80×10^{20} V m^{-2} and 0.24, respectively, after optimization. It was shown that the quadrupolar parameter values obtained for the optimized structures are in better agreement with the experimental values.[17,18] The ^{27}Al and ^{23}Na EFG components were calculated for the optimized structures of $Na_2Ca_3Al_2F_{14}$, α-$NaCaAlF_6$, and β-$NaCaAlF_6$. The deduced ν_Q and η_Q parameters are collected in Table 2. The NMR resonances are then attributed to the corresponding crystallographic sites

Table 3. Line Labels, Relative Intensities (%), and $\delta_{iso,exp}$ (ppm) Values As Deduced from ^{19}F NMR Spectrum Reconstruction, Line Attributions, and $\delta_{iso,cal}$ (ppm) Calculated with the Refined Parameter Set, for the Studied Compounds from the Ternary System $NaF-CaF_2-AlF_3$ and the Basic NaF, CaF_2, and AlF_3 Fluorides[a]

line	relative intensity	$\delta_{iso,exp}$ (±1 ppm)	site	$\delta_{iso,cal}$
		$Na_2Ca_3Al_2F_{14}$		
1	43	−2	**F1**	−7
2	43	16	**F2**	22
3	14	42	**F3**	42
		α-$NaCaAlF_6$		
1	16	−24	**F12**	−28
			F9	−26
2	8	−10	**F6**	−8
3	23	2	F3	0
			F7	0
			F5	2
4	10	8	F11	5
5	15	10	F4	7
			F10	10
6	10	12	F1	19
7	9	22	F8	22
8	9	37	**F2**	45
		β-$NaCaAlF_6$		
1	67	6	F2	2
			F3	6
2	33	13	F1	6
		NaF		
1	100	−57.5	**F1**	−51
		CaF_2		
1	100	58	**F1**	54
		AlF_3		
1	100	−5	**F1**	−1

[a] Unambiguous line attributions are in boldface.

Table 4. Parameters Δd (Å), $\Delta\theta_{||}$ (deg), $\Delta\theta_{\perp}$ (deg) Characterizing the AlF_6^{3-} Octahedron Distortions before (init.) and after Optimization (opt.) of α-$NaCaAlF_6$

	Δd		$\Delta\theta_{||}$		$\Delta\theta_{\perp}$	
site	init.	opt.	init.	opt.	init.	opt.
Al1	0.062	0.032	6.38	7.65	4.41	4.00
Al2	0.068	0.018	10.78	5.04	5.55	2.60

Table 5. Sodium, Aluminum, and Calcium α_l (Å^{-1}), d_0 (Å), and σ_{l_0} (ppm) Parameters: Initially Defined by Bureau et al.,[21] Refined by Body et al.,[22] and Refined in This Work

atom		α_l	d_0	σ_{l_0}
Na	Bureau et al.	3.256	2.317	−11.6
	refined	3.397	2.334	−11.9
Al	Bureau et al.	3.521	1.797	−61.0
	Body et al.	1.737	1.773	−63.1
	refined	2.477	1.806	−61.9
Ca	Bureau et al.	2.976	2.369	−46.3
	Body et al.	3.303	2.353	−46.2
	refined	2.296	2.367	−45.5

by comparing the experimental and calculated quadrupolar parameter values: they are paired to minimize the difference between the calculated and experimental values. The two aluminum and two sodium NMR resonances of α-$NaCaAlF_6$ can, consequently, be assigned to their respective crystallographic sites (Table 2). For all of the compounds, the calculated and experimental ν_Q values are very close, with a maximum difference of less than 10%. The agreement between experimental and calculated η_Q values is also very nice. This agreement is all the more remarkable because the η_Q parameter values strongly depend on the local environment of the considered cation.

2. ^{19}F Superposition Model. 2.1. Presentation of the Model. This model was proposed by Bureau et al.[21] for purely ionic fluorides. The ^{19}F isotropic chemical shift δ_{iso} is considered as a sum of one constant diamagnetic term and several paramagnetic contributions from the neighboring M = Al, Ca, Na cations. The calculation of δ_{iso} can be performed using the main formula of Bureau et al.:[21] $\delta_{iso} = -127.1 - \sum\sigma_l$ with $\sigma_l = \sigma_{l_0} \exp[-\alpha_l(d - d_0)]$. d_0 is the characteristic F−M distance, which is taken to be equal to the bond length in the related basic fluoride (NaF, CaF_2, AlF_3). σ_{l_0} is the parameter that determines the order of magnitude of the cationic paramagnetic contribution to the shielding and was deduced from measurements in the related basic fluoride. For sodium, aluminum, and calcium whose atomic radial wave functions are known, α_l was deduced from the behavior of the cation isotropic paramagnetic contribution. The last step, using the model, is to define the number of neighboring cations M whose contributions have to be taken into account. We decided to consider only atoms included in a sphere of 3.5-Å radius because it was shown that for larger distances the cationic contributions become negligible.[22] The starting parameters that we used in our calculations are those defined by Bureau et al.[21] for Al, Ca, and Na atoms. The isotropic chemical shift values obtained with this model are compared with the experimental results for the $NaF-CaF_2-AlF_3$ ternary system. The calculated and experimental δ_{iso} values are then paired, with regard to the first attribution based on the relative NMR line intensities, to minimize the difference: $\Delta\delta_{iso} = \delta_{iso,exp} - \delta_{iso,cal}$. The rms deviation is 12 ppm, and the maximum difference between measured and calculated δ_{iso} values reaches 32 ppm. Using the parameters refined by Body et al.[22] for Al and Ca atoms gives a slightly better result. The rms deviation is 8 ppm. With the isotropic chemical shift being sensitive to the M−F distances, we applied this initial model using the M−F distances obtained after optimization of the $Na_2Ca_3Al_2F_{14}$, α-$NaCaAlF_6$, and β-$NaCaAlF_6$ structures by the WIEN2k code. We keep the nonoptimized structures for NaF,[42] CaF_2,[43] and AlF_3,[44] whose structure resolution was achieved from crystal X-ray diffraction data. With both parameter sets (from Bureau et al.[21] and from Body et al.[22]), the rms deviation is 6 ppm, and the maximum difference between measured and calculated δ_{iso} values still reaches 19 ppm.

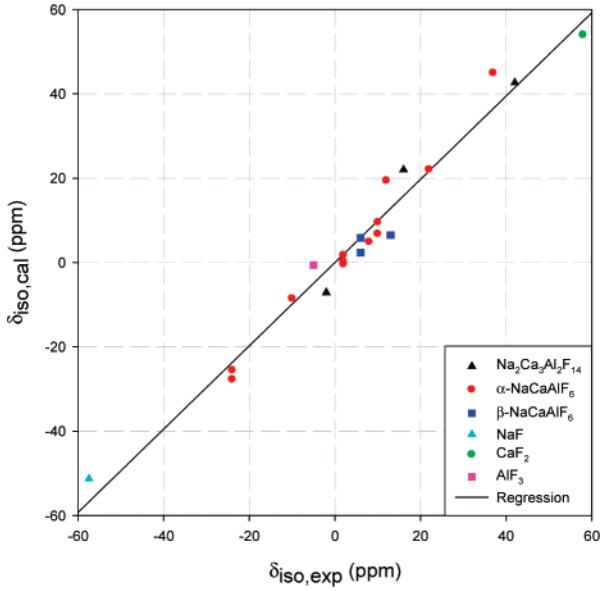

Figure 7. Calculated ^{19}F NMR isotropic chemical shift values versus experimental ones. The solid line corresponds to the linear regression.

2.2. Refinement of the Phenomenological Parameters. To obtain a better agreement between experimental and calculated values, Body et al.[22] previously showed that the three phenomenological parameters α_l, d_0, and σ_{l_0} had to be adjusted for each cation. It is achieved by minimizing the sum $\sum(\delta_{iso,exp} - \delta_{iso,cal})^2$. A new parameter set is obtained, and the line attribution is modified, with respect to the relative intensities, to keep the difference between calculated and experimental δ_{iso} values at a minimum. This process is repeated until the line attribution remains unchanged. Because the first results of the model seemed to be already better with the M−F distances from the optimized structures, we refined the phenomenological parameters using these distances. The starting parameter set (from Bureau et al.[21] or from Body et al.[22]) does not change the result of the calculation. The final parameter set is shown in Table 5. The comparison between experimental and calculated values is plotted in Figure 7 and gives the following result: $\delta_{iso,cal} = 0.987\delta_{iso,exp}$ with a correlation coefficient equal to 0.970. The rms deviation is 4 ppm, and the maximum difference between measured and calculated δ_{iso} values is less than 8 ppm. This very low rms deviation evidences the excellent agreement between calculated and experimental δ_{iso} values and the efficiency of the model. The final line attributions are gathered in Table 3.

(42) Deshpande, V. P. *Acta Crystallogr.* **1961**, *14*, 794−794.
(43) Zhurova, E. A.; Maximov, B. A.; Simonov, V. I.; Sobolev, B. P. *Kristallographiya* **1996**, *41*, 438−443.
(44) Daniel, P.; Bulou, A.; Rousseau, M.; Nouet, J.; Fourquet, J. L.; Leblanc, M.; Burriel, R. *J. Phys.: Condens. Matter* **1990**, *2*, 5663−5677.

Initial and final ^{19}F line attributions remain unchanged for $Na_2Ca_3Al_2F_{14}$ and β-$NaCaAlF_6$. F3, F4, and F11 are inverted for α-$NaCaAlF_6$. Considering that their δ_{iso} calculated values are 2, 8, and 10 ppm, respectively, and that the rms deviation is 4 ppm, the line assignment for these three F atoms is not definite.

2.3. Interpretation of the Phenomenological Parameter Variations. The initial and refined parameter sets are gathered in Table 5. The characteristic distance d_0 varies little (less than 2%) between the initial and refined values and remains close to the M−F (M = Na, Ca, Al) distances found in the basic NaF, CaF_2, and AlF_3 fluorides. The σ_{l_0} parameters also vary little (less than 3%). One can notice that this value is particularly low for the Na atom (3−5 times smaller than those for the Ca and Al atoms). As a consequence, the Na atom has a weak influence on the isotropic chemical shift values compared to the Ca and Al atoms. As was previously observed by Body et al.,[22] the α_l parameter is the most sensitive one. However, it does not vary much for the sodium cation (4%), which confirms the very good approximation of the purely ionic model.[21] The evolution is much stronger for the aluminum and calcium cations. The most important decrease, with regard to the initial parameter set, is for aluminum. It was proposed[22] that the decrease of α_l from the initial purely ionic model value may be related to the covalent character of the Al−F bond. A decrease for the calcium α_l parameter is also observed. However, this behavior is much more difficult to explain. It can be tentatively attributed to the fact that only small Ca−F ($d - d_0$) distances are observed for α-$NaCaAlF_6$. Then it makes the refinement of the α_l parameter less reliable. This refinement evidences the fact that the parameters have to be adjusted for each new studied system, which is understandable: the α_l parameter is sensitive to the electronic cloud surrounding the nuclei. This cloud is strongly influenced by the cation environment, which varies from one compound to another. Efficiently predicting and calculating the ^{19}F δ_{iso} value requires the study of as many compounds as possible for each new system, which might limit the use of this model.

Conclusions

^{27}Al and ^{23}Na NMR SATRAS and 3Q-MAS spectra were recorded for three compounds from the ternary $NaF-CaF_2-AlF_3$ system. The quadrupolar parameters ν_Q and η_Q were extracted from the spectra reconstruction. In parallel, these parameters were calculated using the WIEN2k ab initio code. With a key step in the reliability of these calculations being the optimization of the atom positions in the structure before calculating the quadrupolar parameters, such a method was systematically used for all of the studied compounds. The optimization is more relevant for compounds whose structural determination was performed from X-ray powder diffraction data. Its main effect is the decrease of the AlF_6^{3-} octahedron distortions. The NMR line attribution is then achieved by a comparison of experimental and calculated ν_Q and η_Q values. The agreement between experimental and calculated values is excellent, and all of the aluminum and sodium sites are assigned to their respective crystallographic sites.

High-speed and high-field ^{19}F NMR MAS spectra were acquired for the same compounds. Because the ^{19}F NMR resonance line relative intensities only allow one attribution of the fluorine sites, the superposition model defined by Bureau et al.[21] was used. In a first step, the ^{19}F NMR isotropic chemical shifts were calculated using the parameters initially defined by Bureau et al.[21] for Al, Ca, and Na atoms. Similar calculations were performed using the structures optimized via the WIEN2k calculation code. With the results being better, the phenomenological parameters were then refined using these structures. After refinement of the parameters, the agreement between experimental and calculated δ_{iso} values is very nice, with a 4 ppm rms deviation. The refined parameter set is different from the one initially proposed by Bureau et al.[21] and from the one refined by Body et al.[22] for aluminum and calcium cations. This present work shows one limit of this model: the phenomenological parameters have to be refined for each new studied system. This requires the study of numerous compounds in each system and can become long and fastidious. Now, the PARATEC calculation code[5] allows simultaneous ab initio calculations of isotropic chemical shifts and EFGs.[45,46] Such calculations are in progress on fluoride compounds, and the first results seem to be very promising. The compounds studied in this work are very good candidates to go deeply into these calculations because they are constituted of many multisite nuclei, including quadrupolar nuclei.

Acknowledgment. We thank A.-M. Mercier and Dr. A. Hemon-Ribaud, from the Laboratoire des Oxydes et Fluorures, who supplied us with $Na_2Ca_3Al_2F_{14}$ and β-$NaCaAlF_6$.

Supporting Information Available: Atomic coordinates of the initial and WIEN2k-optimized structures of $Na_2Ca_3AlF_{14}$, α-$NaCaAlF_6$, and β-$NaCaAlF_6$. This material is available free of charge via the Internet at http://pubs.acs.org.

IC061348J

(45) Profeta, M.; Mauri, F.; Pickard, C. J. *J. Am. Chem. Soc.* **2003**, *125*, 541−548.
(46) Gervais, C.; Profeta, M.; Babonneau, F.; Pickard, C. J.; Mauri, F. *J. Phys. Chem. B* **2004**, *108*, 13249−13253.